

# Fluorescent properties of DNA base analogue tC upon incorporation into DNA — negligible influence of neighbouring bases on fluorescence quantum yield

Peter Sandin, L. Marcus Wilhelmsson\*, Per Lincoln, Vicki E. C. Powers<sup>1</sup>, Tom Brown<sup>1</sup> and Bo Albinsson

Physical Chemistry Section, Department of Chemistry and Bioscience, Chalmers University of Technology, SE-41296 Gothenburg, Sweden and <sup>1</sup>School of Chemistry, University of Southampton, Highfield, Southampton SO17 1BJ, UK

Received June 15, 2005; Revised and Accepted August 9, 2005

## ABSTRACT

The quantum yield of the fluorescent tricyclic cytosine analogue, 1,3-diaza-2-oxophenothiazine, tC, is high and virtually unaffected by incorporation into both single- and double-stranded DNA irrespective of neighbouring bases (0.17–0.24 and 0.16–0.21, respectively) and the corresponding fluorescence decay curves are all mono-exponential, properties that are unmatched by any base analogue so far. The fluorescence lifetimes increase when going from tC free in solution (3.2 ns) to single- and double-stranded DNA (on average 5.7 and 6.3 ns, respectively). The mono-exponential decays further support previous NMR results where it was found that tC has a well-defined position and geometry within the DNA helix. Furthermore, we find that the oxidation potential of tC is 0.4 V lower than for deoxyguanosine, the natural base with the lowest oxidation potential. This suggests that tC may be of interest in charge transfer studies in DNA as an electron hole acceptor. We also present a novel synthetic route to the phosphoramidite form of tC. The results presented here together with previous work show that tC is a very good C-analogue that induces minimal perturbation to the native structure of DNA. This makes tC unique as a fluorescent base analogue and is thus highly interesting in a range of applications for studying e.g. structure, dynamics and kinetics in nucleic acid systems.

## INTRODUCTION

The ability to detect emission at the single molecule level (1) makes fluorescence one of the most sensitive analytical techniques available today. Fluorescence spectroscopy has been widely used in nucleic acid research to study structure and dynamics as well as the kinetics of interactions between DNA and other molecules. In this context fluorescent base analogues are particularly interesting [see Rist and Marino (2) for a recent review]. The analogues are very similar in both size and shape to the naturally occurring bases, giving them one important property: the potential to be incorporated into DNA at specific sites with minimal disturbance to the overall structure. Two other important requirements of fluorescent base analogues are their ability to form specific base pairs and to have a sufficiently high fluorescence quantum yield when incorporated into DNA. Fluorophores with these properties provide a unique opportunity to incorporate a probe into the stacked region of DNA close to the site of interest with minimal perturbation to the native DNA structure. Because of the stacking of the base analogue, independent movement relative to the overall complex is highly restricted, resulting in a very well-defined geometry. These are important properties for fluorescence anisotropy and fluorescence resonance energy transfer (FRET) studies.

The most commonly used fluorescent base analogue, 2-aminopurine (2-AP) (3–5), forms stable base pairs with thymine but also moderately stable base pairs with cytosine (6–9), and the high fluorescence quantum yield of 2-AP free in solution (0.68) is considerably reduced (~100 times but highly dependent on base sequence) when incorporated into nucleic acids (4). This sensitivity to the microenvironment has been

\*To whom the correspondence should be addressed. Tel: +46 31 7723051; Fax: +46 31 7723858; Email: marcus.wilhelmsson@chalmers.se

utilized in studies of e.g. structure and dynamics within both DNA and RNA (10,11), dynamics and kinetics of DNA–protein interaction (12–17) and electron transfer within DNA (18–21). However, the less efficient and less specific base pairing relative to adenine introduces a perturbation to the native structure of DNA and also gives 2-AP increased dynamics within the DNA helix. This, in combination with the sensitivity of the fluorescence quantum yield to the environment, makes 2-AP less suited as a probe for studies of molecular dynamics and DNA–protein interaction using fluorescence anisotropy and FRET.

Other commercially available fluorescent base analogues are the pteridine analogues of guanine (3-MI and 6-MI) (22–24) and adenine (6MAP and DMAP) (25) [see Hawkins (26) for a recent review]. Like 2-AP, these probes are very sensitive to the microenvironment and are highly quenched, with fluorescence quantum yields ranging from <0.01 to 0.3 depending on the nature of the surrounding base pairs, when incorporated into DNA (23,25). Furthermore, duplex melting temperature studies have shown that with the exception of 6-MI, they reduce the thermal stability of oligonucleotides (23,25). For example, incorporation of 3-MI is approximately equivalent to a single base pair mismatch (23). Other fluorescent base analogues have also been used and studied. They are all either highly quenched when incorporated into DNA or cause a destabilization of the DNA duplex, or both (4,27–35).

Recently we have reported the interesting fluorescent properties of the base analogue 1,3-diaza-2-oxophenothiazine, tC (Figure 1), as a monomer (36) and when incorporated into a peptide nucleic acid (PNA)-sequence where tC was positioned between a T and an A (37). The fluorescence quantum yield was virtually unaffected upon incorporation of tC into this specific PNA single-stranded sequence and also upon subsequent hybridization to its complementary DNA single-strand (37). We have also shown that an acetic acid derivative of tC (KtC, Figure 1) exists as its normal base-pairing tautomer in the pH range 4–12 and exhibits a high fluorescence quantum yield (~0.2) in aqueous solution (36). Previous reports have shown that tC discriminates well between A and G targets and

that it thermally stabilizes DNA–DNA-, DNA–RNA-, PNA–DNA-, PNA–RNA- and PNA–PNA-duplexes (38–42). The stabilization is most probably due to the improved stacking between the natural bases and the three-ring structure of tC. In a recent study we used UV-melting, circular dichroism and NMR to investigate how the exchange of cytosine for tC in DNA influences local conformation, overall structure and duplex stability (42). The study showed that incorporation of tC leaves the DNA virtually unaffected in an overall B-form and that G:tC base pairs show no increased dynamics as compared with the normal base pairs. All these observations suggest that tC is a good base analogue for C. However, the influence of size and electronic character of the more extended ringsystem of tC compared with C when it comes to interactions between tC-modified DNA and proteins has still not been examined in detail and will be an important matter to investigate in the future.

The tC-base has its lowest energy electronic transition at ~375 nm (36), which is well separated from the transitions of the natural DNA bases and amino acids, and can therefore be selectively excited even in the presence of other DNA and protein chromophores. Previous work has shown this absorption band to be the result of a single transition moment directed ~35° from the long axis of tC (36). The absorption maximum of tC overlaps well with tryptophan emission making it possible to use tC as an acceptor of tryptophan emission in FRET experiments. We have also shown that tC serves as an excellent FRET donor with rhodamine as an acceptor (37). The unique fluorescence properties of the tC base, together with the rigid and well-defined geometry and orientation expected for tC stacked within the DNA duplex, will be a major advantage for FRET experiments to accurately measure distances within macromolecular systems, and in fluorescence anisotropy measurements.

The fluorescence quantum yield of all fluorescent base analogues in use today shows large variations depending on neighbouring bases. Previous studies of the fluorescence quantum yield of tC in nucleic acid only include one example of a PNA single-stranded sequence with T and A as closest neighbouring bases and its corresponding PNA–DNA duplex (37). We now report on the influence of all possible nearest neighbour nucleobase variations, disregarding 5'–3'-directionality, on fluorescence properties of tC incorporated into DNA oligomers. The investigation of the fluorescence properties is crucial for the future use of this promising base analogue. Fluorescence quantum yields and lifetimes for tC in both single- and double-stranded DNA are presented and show very stable fluorescence properties for tC. We also report the redox potentials of tC which suggest a new property that may be used in electron transfer studies in nucleic acid systems. Furthermore, we present a novel synthetic route to the phosphoramidite form of tC.

## MATERIALS AND METHODS

### Chemicals

Standard buffer in all measurements, unless stated otherwise, was a sodium phosphate buffer, pH 7.5, with a total sodium concentration of 50 mM. The potassium salt of 1,3-diaza-2-oxophenothiazin-3-yl acetic acid (KtC) (Figure 1) was

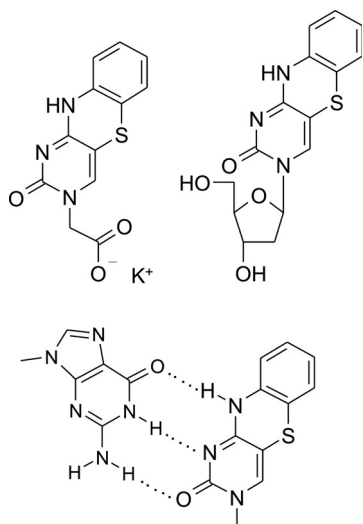
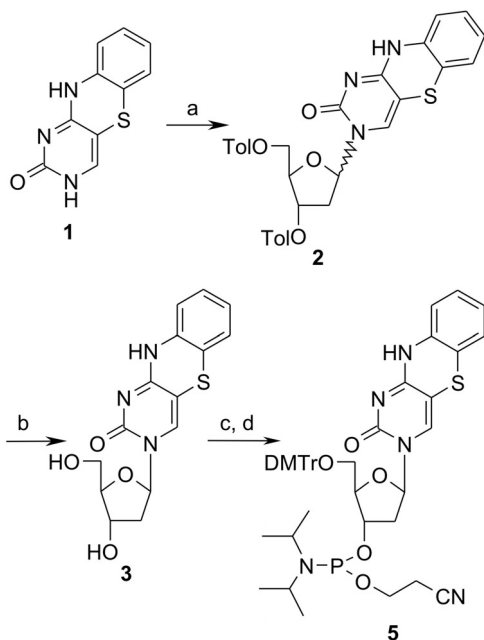


**Figure 1.** Structure of potassium salt of the acetic acid derivative of tC (KtC) upper left, tC nucleoside (tCnuc) upper right and G:tC base pair below.



**Scheme 1.** Synthesis of the tC phosphoramidite. Reagents and conditions: (a) (i) 1.1 eq. NaH in DMF, RT, (ii) 1.1 eq. 2-deoxy-3,5-di-*O*-*p*-toluoyl- $\alpha$ -D-erythro-pentofuranosyl chloride, 2 h, RT; (b) 1 eq. NaOMe in methanol, RT, 14% from 1; (c) 1.1 eq. 4,4'-dimethoxytrityl chloride in pyridine, 2 h, RT, 70%; (d) 1.5 eq. 2-cyanoethyl-*N,N*-diisopropylchlorophosphoramidite, 2.5 eq. diisopropylethylamine in anhydrous tetrahydrofuran, 30 min, RT, 94%.

synthesized from the methyl ester, which was obtained by alkylation of the anion of 1,3-diaza-2-oxophenothiazine (43,44) with methylbromoacetate, following the general procedure of Eldrup *et al.* (38).

#### Synthesis of 3-[2-deoxy-3-*O*-[2-cyanoethoxy-*N,N*-diisopropylamino]-phosphino]-5-*O*-(4,4'-dimethoxytrityl)- $\beta$ -D-ribofuranosyl]-1,3-diaza-2-oxophenothiazine (5)

3-(2-Deoxy- $\beta$ -D-ribofuranosyl)-1,3-diaza-2-oxophenothiazine (3) was synthesized from 1,3-diaza-2-oxophenothiazine (1) as shown in Scheme 1. The sodium salt of 1, produced *in situ* with sodium hydride in dimethyl formamide (DMF) was treated with 2-deoxy-3,5-di-*O*-*p*-toluoyl- $\alpha$ -D-erythro-pentofuranosyl chloride (45) at room temperature for 2 h to yield the toluoyl-protected nucleoside (2) as an anomeric mixture. Both anomers were deprotected and separated on a silica column. Dimethoxytritylation at the 5'-OH group and conversion to the 3'-*O*-phosphoramidite of the  $\beta$ -anomer were carried out in the conventional manner and afforded the phosphoramidite monomer (5). (For more details see Supplementary Data.)

#### Oligodeoxyribonucleotide synthesis

Oligonucleotides containing tC were synthesized on an ABI 394 DNA/RNA synthesizer on the 0.2  $\mu$ M scale by standard automated solid-phase methods using  $\beta$ -cyanoethyl phosphoramidites. Cleavage from the solid support and deprotection was carried out in the normal manner using concentrated aqueous ammonia at 55°C for 5 h. Oligonucleotides were purified by reversed-phase high-performance liquid chromatography on a C8 (octyl) column, eluting with a gradient

of 0.1 M ammonium acetate to 25% acetonitrile in 0.1 M ammonium acetate buffer (46). Desalting was carried out by Sephadex gel-filtration (Nap 10, Pharmacia). Normal oligonucleotides, not containing tC, were purchased from Eurogentec.

#### Concentration determination

Concentrations of oligonucleotides were determined by UV absorption measurements at 260 nm. The extinction coefficients for the modified oligonucleotides were approximated by linear combinations of extinction coefficients of the natural nucleotides and the extinction coefficient of the potassium salt of 1,3-diaza-2-oxophenothiazin-3-yl acetic acid (KtC) (Figure 1). To account for the base-stacking interactions, this linear combination was multiplied by 0.9 to give the final extinction coefficients for the oligomers. The individual extinction coefficients, at 260 nm, used were  $\epsilon_T = 9300 \text{ M}^{-1} \text{ cm}^{-1}$ ,  $\epsilon_C = 7400 \text{ M}^{-1} \text{ cm}^{-1}$ ,  $\epsilon_G = 11800 \text{ M}^{-1} \text{ cm}^{-1}$ ,  $\epsilon_A = 15300 \text{ M}^{-1} \text{ cm}^{-1}$  (47) and  $\epsilon_{\text{KtC}} = 13500 \text{ M}^{-1} \text{ cm}^{-1}$ . This resulted in the following extinction coefficients at 260 nm for the modified oligonucleotides:  $\epsilon_{\text{TA}} = 97650 \text{ M}^{-1} \text{ cm}^{-1}$ ,  $\epsilon_{\text{AA}} = 103050 \text{ M}^{-1} \text{ cm}^{-1}$ ,  $\epsilon_{\text{TT}} = 92250 \text{ M}^{-1} \text{ cm}^{-1}$ ,  $\epsilon_{\text{GA}} = 99900 \text{ M}^{-1} \text{ cm}^{-1}$ ,  $\epsilon_{\text{CT}} = 90540 \text{ M}^{-1} \text{ cm}^{-1}$ ,  $\epsilon_{\text{TG}} = 94500 \text{ M}^{-1} \text{ cm}^{-1}$ ,  $\epsilon_{\text{CA}} = 95940 \text{ M}^{-1} \text{ cm}^{-1}$ ,  $\epsilon_{\text{GG}} = 96750 \text{ M}^{-1} \text{ cm}^{-1}$ ,  $\epsilon_{\text{CC}} = 88830 \text{ M}^{-1} \text{ cm}^{-1}$  and  $\epsilon_{\text{GC}} = 92790 \text{ M}^{-1} \text{ cm}^{-1}$  (indices of  $\epsilon$ s as in Table 1). Extinction coefficients for the purchased oligonucleotides were used as given by Eurogentec.

#### Hybridization of duplex oligodeoxyribonucleotides

Solutions of tC-containing single-strands were mixed at room temperature with solutions containing a 20% excess of their complementary strands. Samples were heated to 90°C and thereafter annealed by slow cooling to 25°C.

#### Fluorescence measurements

Fluorescence quantum yields of the different tC-containing oligonucleotides were determined relative to the quantum yield of 9,10-diphenylanthracene in degassed ethanol ( $\Phi_f = 0.95$ ) (48). The measurements were performed on a SPEX fluorolog 3 spectrofluorimeter (JY Horiba) using emission wavelengths between 397 and 750 nm and an excitation wavelength of 393 nm.

Fluorescence lifetimes were determined using time-correlated single photon counting. The samples were excited with a PicoQuant PLS-8-2-060 pulsed diode with an approximate centre wavelength of 370 nm (FWHM 50 nm). The diode was pulsed at a 20 MHz repetition rate with a pulse width of  $\sim 1$  ns and the emission was monitored at 500 nm. The photons were collected by a microchannel-plate photomultiplier tube (MCP-PMT R3809U-50; Hamamatsu) and fed into a multi-channel analyser with 4096 channels. A minimum of 10 000 counts were recorded in the top channel. The intensity data were convoluted with the instrument response and evaluated with the software package F900. The experimental setup yielded a time resolution of  $\sim 100$  ps (FWHM).

#### Electrochemistry

Experiments were performed on a CH Instruments Model 650A electrochemical workstation, with a three-electrode

**Table 1.** Fluorescence quantum yields, fluorescence lifetimes, radiative rate constants, wavelength of emission maxima and of the lowest energy absorption band maxima for tC-containing single-stranded oligonucleotides and the monomers, KtC<sup>d</sup> and tCnuc<sup>d</sup>

DNA sequence	Neighbouring bases = name of oligomer	$\Phi_f^{a,b}$	$\tau/\text{ns}^a$	$k_f/10^7\text{s}^{-1}^c$	$\text{Em}_{\text{max}}/\text{nm}^a$	$\text{Abs}_{\text{max}}/\text{nm}^a$
5'-CGC-AGtC-ATC-G-3'	GA	0.17	5.3	3.2	513	402
5'-CGC-ACtC-TTC-G-3'	CT	0.21	5.6	3.8	509	390
5'-CGC-AGtC-CTC-G-3'	GC	0.19	5.3	3.6	509	394
5'-CGC-ACtC-ATC-G-3'	CA	0.20	5.6	3.6	510	392
5'-CGC-AGtC-GTC-G-3'	GG	0.18	5.4	3.3	510	399
5'-CGC-ACtC-CTC-G-3'	CC	0.22	5.9	3.7	508	392
5'-CGC-ATtC-ATC-G-3'	TA	0.21	5.8	3.6	509	390
5'-CGC-AAtC-ATC-G-3'	AA	0.21	5.6	3.8	510	391
5'-CGC-ATtC-TTC-G-3'	TT	0.22	5.7	3.9	507	390
5'-CGC-ATtC-GTC-G-3'	TG	0.24	6.5	3.7	506	391
KtC <sup>d</sup>		0.16	3.8	4.2	506	375
tCnuc <sup>d</sup>		0.13	3.2	4.1	513	377

<sup>a</sup>Measurements performed in phosphate buffer (50 mM Na<sup>+</sup>, pH 7.5) at room temperature.

<sup>b</sup>Fluorescence quantum yields measured relative to the quantum yield of 9,10-diphenylanthracene in ethanol ( $\Phi_f = 0.95$ ) (48).

<sup>c</sup>Radiative rate constant  $k_f = \Phi_f/\tau$ .

<sup>d</sup>KtC is the potassium salt of the acetic acid derivative of tC (Figure 1) and tCnuc is the nucleoside derivative of tC (Figure 1).

configuration [Pt wire counter electrode, glassy carbon working electrode, polished with 0.05  $\mu\text{m}$  alumina paste, immersed in concentrated HNO<sub>3</sub> for 1 min and washed with ethanol prior to the experiments, and Ag/AgCl reference electrode (0.2 V versus NHE)]. Buffer used in each experiment was a 0.1 M sodium phosphate buffer at pH 5.5. Both differential pulse voltammetry and cyclic voltammetry were used to determine the oxidation and reduction potential and K<sub>3</sub>[Fe(CN)<sub>6</sub>] was used as an external standard.

## RESULTS

For future fluorescence-based applications, it is very important to understand the properties of tC when incorporated into different DNA sequence environments. A previous study of tC incorporated into a PNA sequence (T and A as closest neighbouring bases to tC) showed that the fluorescence quantum yield of tC is stable when going from its monomeric form to this specific nucleobase environment (37). However, we still needed to investigate the effect of surrounding base pairs on the quantum yield of tC in both single- and double-stranded DNA. This was done by studying 10 different DNA decamers both as single- and double-strands, the only difference between the decamers being the two bases flanking tC. The 10 decamers cover all possible nearest neighbour variations for tC, disregarding 5'-3'-directionality.

Figure 2 shows the normalized absorption and emission spectra for the tC nucleoside (tCnuc) and one example of a spectrum of a tC-modified single- and double-stranded oligomer, respectively. The lowest energy absorption maxima for single- (dashed line) and double-strands (dotted line) are red shifted compared with the monomer (375 nm, solid line) and range from 390 to 402 nm and 389 to 399 nm, respectively. Their emission maxima range from 506 to 513 nm and 502 to 507 nm, respectively. Emission profiles of the monomers, KtC and tCnuc, and the single- and double-strands are very similar. However, both single- and double-strands show shoulders at  $\sim 480$  and  $525$  nm and  $485$  and  $525$  nm, respectively, on both sides of the emission maxima (Figure 2). The shoulders are more pronounced for double-strands and are more difficult to detect in the single-strands. These shoulders also appear in the

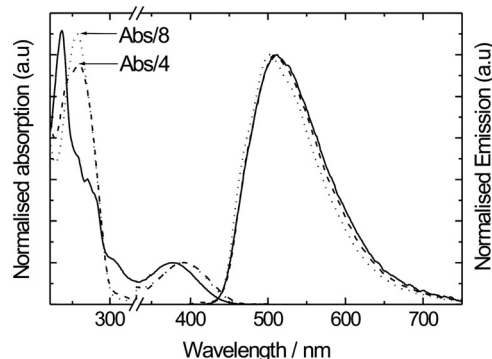


**Figure 2.** Examples of absorption and emission spectra of tCnuc (solid lines), tC-containing single-strand (CA, dashed lines) and tC-containing double-strand (CA, dotted lines) normalized at the maxima of the lowest energy absorption band (left) and of the emission (right), respectively.

emission profile for tC in a H<sub>2</sub>O/ethylene glycol glass at  $-100^\circ\text{C}$  (data not shown).

Emission and absorption properties for the 10 different single- and double-stranded oligonucleotides are listed in Tables 1 and 2, respectively. The data show high and stable quantum yields for tC in both single- (0.17–0.24) and double-stranded oligonucleotides (0.16–0.21). The average fluorescence quantum yield of the single-strands is slightly higher (0.21) than that of the double-strands (0.19). The quantum yields of the monomers, KtC and tCnuc, are also included in Table 1. These quantum yields have previously been slightly overestimated due to that the reference sample was not degassed, resulting in an underestimation of the value for the reference emission.

Time-dependent emission decay curves for all decamers could, with the time resolution of the experimental setup, be fitted to single exponential curves ( $\chi_r^2 < 1.2$ ) with fluorescence lifetimes ranging from 5.3 to 6.5 ns for single-strands and from 5.7 to 6.9 ns for double-strands. The average fluorescence lifetime for double-strands is in general slightly longer, as compared with single-strands, while as mentioned above, the average fluorescence quantum yield is slightly lower. Also shown in the tables are the radiative rate constant,

**Table 2.** Fluorescence quantum yields, fluorescence lifetimes, radiative rate constants, wavelength of emission maxima and of the lowest energy absorption band maxima for tC-containing double-stranded oligonucleotides

DNA sequence	Neighbouring bases = name of oligomer	$\Phi_f^{a,b}$	$\tau/\text{ns}^a$	$k_f/10^7\text{s}^{-1}^c$	$\text{Em}_{\text{max}}/\text{nm}^a$	$\text{Abs}_{\text{max}}/\text{nm}^a$
5'-CGC-AGtC-ATC-G-3'	GA	0.18	5.9	3.1	505	389
5'-CGC-ACtC-TTC-G-3'	CT	0.20	6.6	3.0	502	395
5'-CGC-AGtC-CTC-G-3'	GC	0.16	5.7	2.8	507	391
5'-CGC-ACtC-ATC-G-3'	CA	0.20	6.6	3.0	502	391
5'-CGC-AGtC-GTC-G-3'	GG	0.18	6.3	2.9	506	391
5'-CGC-ACtC-CTC-G-3'	CC	0.19	6.4	3.0	503	393
5'-CGC-ATtC-ATC-G-3'	TA	0.20	6.5	3.1	503	395
5'-CGC-AAtC-ATC-G-3'	AA	0.18	5.9	3.1	507	392
5'-CGC-ATtC-TTC-G-3'	TT	0.20	6.5	3.1	503	399
5'-CGC-ATtC-GTC-G-3'	TG	0.21	6.9	3.0	503	397

<sup>a</sup>Measurements performed in phosphate buffer (50 mM Na<sup>+</sup>, pH 7.5) at room temperature.

<sup>b</sup>Fluorescence quantum yields measured relative to the quantum yield of 9,10-diphenylanthracene in ethanol ( $\Phi_f = 0.95$ ) (48).

<sup>c</sup>Radiative rate constant  $k_f = \Phi_f/\tau$ .

$k_f$ , for each decamer. This value is virtually constant within the two groups (single- and double-strands) showing a slightly higher average for the single-strands ( $3.7 \times 10^7 \text{ s}^{-1}$ ) compared with the double-strands ( $3.0 \times 10^7 \text{ s}^{-1}$ ). Both of these averages are smaller than the radiative rate constant of the tCnuc ( $4.1 \times 10^7 \text{ s}^{-1}$ ).

One-electron-redox potentials in sodium phosphate buffer solution, pH 5.5, were measured with both cyclic voltammetry and differential pulse voltammetry. The oxidation potential for tCnuc was 0.9 V and the reduction potential  $-1.1$  V. With the same experimental setup the oxidation potential for deoxyguanosine (dG) was determined to be 1.4 V, which agrees well with values reported in literature (49,50).

## DISCUSSION

In earlier studies we have shown that the fluorescence quantum yield of tC is remarkably stable and virtually unaffected by incorporation into a single-stranded sequence of PNA and the corresponding PNA–DNA duplex with T and A as neighbouring bases (37). Recently we have also shown that tC incorporated into an oligonucleotide context forms specific base pairs with guanine with no increased dynamics, such as base pair opening or flipping between syn/anti conformation, as compared with the natural bases (42). These results are further supported in the present study. The work shows that the fluorescence quantum yields and fluorescence lifetimes, of the base analogue, tC, are virtually unaffected by incorporation into DNA single- and double-strands regardless of the nature of the neighbouring bases (Tables 1 and 2), which is a unique property of a fluorescent DNA base analogue [cf. review by Rist and Marino (2)]. We observe an average decrease in radiative rate constant,  $k_f$ , for the free tCnuc ( $k_f = 4.1 \times 10^7 \text{ s}^{-1}$ ) when incorporated into single-stranded DNA ( $k_f = 3.7 \times 10^7 \text{ s}^{-1}$ ) and a further decrease when incorporated into double-stranded DNA ( $k_f = 3.0 \times 10^7 \text{ s}^{-1}$ ). This variation and also the small variation within each group (3.2–3.9 and 2.8–3.1 for single- and double-strands, respectively) can be explained by the Strickler–Berg theorem (51), which states that the radiative rate constant for fluorescence is directly proportional to the probability of the corresponding absorption process, i.e. proportional to the area under the lowest absorption band. Stacking of the bases in DNA leads

to hypochromicity which results in a lower extinction coefficient which, in turn, according to Strickler–Berg, results in a lowered radiative rate constant. The hypochromicity depends on how well the base is stacked within DNA, on the surrounding bases and also on whether the strand is hybridized to a complementary strand or not. Although the hypochromicity for the low energy absorption band of tC in single- and double-stranded DNA has not been quantified, it is reasonable to assume that it will behave similarly to the natural DNA bases, which show up to a 25% decrease in absorption in single-stranded DNA and up to a 40% decrease in absorption in double-stranded DNA as compared with monomeric nucleotides (52). The decreases in radiative rate constant for tCnuc incorporated into single- and double-stranded DNA are in the ranges 5–22% and 24–31%, respectively, as compared with tCnuc. This suggests that hypochromicity might very well be the explanation for the differences in radiative rate constant in all the samples. As a consequence, this conclusion indicates that the non-radiative rate constants,  $k_{ic}$  and  $k_{isc}$ , are virtually constant in all samples.

Although the limited time resolution of the experimental setup prevents us from detecting short lifetimes (sub-nanosecond), the single, well-defined fluorescence lifetime of tC we find in both single- and double-strands is a strong indication that the conformation of tC is fixed and does not exist as a set of different conformations. This further supports the theory that tC does not show increased dynamics in DNA but is well stacked and has no enhanced tendency for base pair opening and flipping as compared with the natural bases. Additional indicators of a rigid environment for tC in DNA are the virtually identical (except for a shift in wavelength maxima), more structured emission profiles for tC when incorporated into single- as well as double-stranded DNA (Figure 2) and the emission profile of tC in a rigid environment like H<sub>2</sub>O/ethylene glycol glass at  $-100^\circ\text{C}$  (data not shown). The fluorescence lifetimes (5.3–6.9 ns) are very well suited for fluorescence anisotropy measurements of oligonucleotides and oligonucleotide–protein complexes. Preliminary results show that tC can be used to follow rotational dynamics on up to at least 50mer single- and double-stranded oligonucleotides and oligonucleotide–protein complexes.

The oxidation potential for tC was found to be 0.9 V in sodium phosphate buffer solution, pH 5.5, which is  $\sim 0.4$  V lower than values reported in literature for dG (49,50) which is

the natural DNA base with the lowest oxidation potential. This suggests that tC might be used as an electron hole acceptor in charge transfer studies in DNA. Furthermore, the reduction potential for tC is  $-1.1$  V which together with the excitation energy for the lowest singlet excited state (2.9 eV) [calculated as the mean of the emission and absorption wavenumber,  $E_{00}(\text{tC}^*) = (26700 + 19600)/2 = 23150 \text{ cm}^{-1} \cong 2.9 \text{ eV}$ ] gives a reduction potential in the excited state of 1.8 V [reduction potential in the excited state,  $E^0(\text{tC}^*/\text{tC}^{\bullet-}) = E^0(\text{tC}/\text{tC}^{\bullet-}) + E_{00}(\text{tC}^*)$ ]. This value is  $\sim 0.3$  V larger than the excited state reduction potential reported for 2-AP (1.5 V) (18). Thus, for thermodynamic reasons tC should be more easily quenched by electron transfer from a nearby base than 2-AP. This is quite surprising, since several studies have claimed that 2-AP is selectively quenched by electron transfer from the guanine base, both in solution and in oligonucleotides (19,20,53). On the other hand, it should be noted that in a recent paper, Reynisson and Steenken (54) showed that excited 2-AP is incapable of oxidizing guanine in solution, thus suggesting that electron transfer does not quench 2-AP, in which case it is less surprising that tC is not quenched by electron transfer. However, if 2-AP is quenched by electron transfer from guanine and tC is not, either in oligonucleotides (irrespective of the neighbouring base) or by dGMP in solution (see Supplementary Figure S1), there must exist other barriers for the electron transfer reaction of tC with the natural bases. One such difference between 2-AP and tC might be follow-up reactions, including prototropic equilibria, which are notoriously sensitive to solvent environment and known to affect the redox potentials for the natural bases (55).

In conclusion, the properties presented in this paper, together with previous results showing that tC induces minimal perturbation to the DNA helix (42), make tC unique as a fluorescent base analogue and very promising as a fluorescent probe in techniques such as fluorescent anisotropy and FRET in nucleic acid studies and also suggests that in the future tC may be of interest for electron transfer studies in DNA.

## SUPPLEMENTARY DATA

Supplementary Data is available at NAR Online.

## ACKNOWLEDGEMENTS

Mikael Winters is gratefully acknowledged for his help in the electrochemistry measurements. This project was funded by the Swedish Research Council (VR) and the Swedish Foundation for Strategic Research (SSF). V.E.C.P. was funded by the BBSRC (UK). Funding to pay the Open Access publication charges for this article was provided by Swedish Research Council (VR).

*Conflict of interest statement.* None declared.

## REFERENCES

- Ha, T. (2001) Single-molecule fluorescence methods for the study of nucleic acids. *Curr. Opin. Struct. Biol.*, **11**, 287–292.
- Rist, M.J. and Marino, J.P. (2002) Fluorescent nucleotide base analogs as probes of nucleic acid structure, dynamics and interactions. *Curr. Org. Chem.*, **6**, 775–793.
- Holmén, A., Nordén, B. and Albinsson, B. (1997) Electronic transition moments of 2-aminopurine. *J. Am. Chem. Soc.*, **119**, 3114–3121.
- Ward, D.C., Reich, E. and Stryer, L. (1969) Fluorescence studies of nucleotides and polynucleotides. I. Formycin 2-aminopurine riboside 2,6-diaminopurine riboside and their derivatives. *J. Biol. Chem.*, **244**, 1228–1237.
- Rachofsky, E.L., Osman, R. and Ross, J.B.A. (2001) Probing structure and dynamics of DNA with 2-aminopurine: effects of local environment on fluorescence. *Biochemistry*, **40**, 946–956.
- Sowers, L.C., Boulard, Y. and Fazakerley, G.V. (2000) Multiple structures for the 2-aminopurine-cytosine mismatch. *Biochemistry*, **39**, 7613–7620.
- Sowers, L.C., Shaw, B.R., Veigl, M.L. and Sedwick, W.D. (1987) DNA-base modification: ionized base pairs and mutagenesis. *J. Biol. Chem.*, **262**, 201–218.
- Sowers, L.C., Fazakerley, G.V., Eritja, R., Kaplan, B.E. and Goodman, M.F. (1986) Base pairing and mutagenesis: observation of a protonated base pair between 2-aminopurine and cytosine in an oligonucleotide by proton NMR. *Proc. Natl Acad. Sci. USA*, **83**, 5434–5438.
- Freese, E. (1959) Specific mutagenic effect of base analogues on phage-T4. *J. Mol. Biol.*, **1**, 87–105.
- Guest, C.R., Hochstrasser, R.A., Sowers, L.C. and Millar, D.P. (1991) Dynamics of mismatched base pairs in DNA. *Biochemistry*, **30**, 3271–3279.
- Stivers, J.T. (1998) 2-Aminopurine fluorescence studies of base stacking interactions at abasic sites in DNA: metal-ion and base sequence effects. *Nucleic Acids Res.*, **26**, 3837–3844.
- Allan, B.W. and Reich, N.O. (1996) Targeted base stacking disruption by the EcoRI DNA methyltransferase. *Biochemistry*, **35**, 14757–14762.
- Bloom, L.B., Otto, M.R., Beechem, J.M. and Goodman, M.F. (1993) Influence of 5'-nearest neighbors on the insertion kinetics of the fluorescent nucleotide analog 2-aminopurine by Klenow fragment. *Biochemistry*, **32**, 11247–11258.
- Hochstrasser, R.A., Carver, T.E., Sowers, L.C. and Millar, D.P. (1994) Melting of a DNA helix terminus within the active-site of a DNA-polymerase. *Biochemistry*, **33**, 11971–11979.
- Lycksell, P.O., Gräslund, A., Claessens, F., McLaughlin, L.W., Larsson, U. and Rigler, R. (1987) Base pair opening dynamics of a 2-aminopurine substituted EcoRI restriction sequence and its unsubstituted counterpart in oligonucleotides. *Nucleic Acids Res.*, **15**, 9011–9025.
- Nordlund, T.M., Andersson, S., Nilsson, L., Rigler, R., Gräslund, A. and McLaughlin, L.W. (1989) Structure and dynamics of a fluorescent DNA oligomer containing the EcoRI recognition sequence: fluorescence, molecular dynamics, and NMR studies. *Biochemistry*, **28**, 9095–9103.
- Stivers, J.T., Pankiewicz, K.W. and Watanabe, K.A. (1999) Kinetic mechanism of damage site recognition and uracil flipping by *Escherichia coli* uracil DNA glycosylase. *Biochemistry*, **38**, 952–963.
- Kelley, S.O. and Barton, J.K. (1999) Electron transfer between bases in double helical DNA. *Science*, **283**, 375–381.
- O'Neill, M.A., Becker, H.C., Wan, C.Z., Barton, J.K. and Zewail, A.H. (2003) Ultrafast dynamics in DNA-mediated electron transfer: base gating and the role of temperature. *Angew. Chem. Int. Ed. Engl.*, **42**, 5896–5900.
- Shafirovich, V., Dourandin, A., Huang, W.D., Luneva, N.P. and Geacintov, N.E. (2000) Electron transfer at a distance induced by site-selective photoionization of 2-aminopurine in oligonucleotides and investigated by transient absorption techniques. *Phys. Chem. Chem. Phys.*, **2**, 4399–4408.
- Wan, C.Z., Fiebig, T., Schiemann, O., Barton, J.K. and Zewail, A.H. (2000) Femtosecond direct observation of charge transfer between bases in DNA. *Proc. Natl Acad. Sci. USA*, **97**, 14052–14055.
- Hawkins, M.E., Pfeleiderer, W., Mazumder, A., Pommier, Y.G. and Falls, F.M. (1995) Incorporation of a fluorescent guanosine analog into oligonucleotides and its application to a real time assay for the HIV-1 integrase 3'-processing reaction. *Nucleic Acids Res.*, **23**, 2872–2880.
- Hawkins, M.E., Pfeleiderer, W., Balis, F.M., Porter, D. and Knutson, J.R. (1997) Fluorescence properties of pteridine nucleoside analogs as monomers and incorporated into oligonucleotides. *Anal. Biochem.*, **244**, 86–95.
- Driscoll, S.L., Hawkins, M.E., Balis, F.M., Pfeleiderer, W. and Laws, W.R. (1997) Fluorescence properties of a new guanosine analog incorporated into small oligonucleotides. *Biophys. J.*, **73**, 3277–3286.
- Hawkins, M.E., Pfeleiderer, W., Jungmann, O. and Balis, F.M. (2001) Synthesis and fluorescence characterization of pteridine adenosine

- nucleoside analogs for DNA incorporation. *Anal. Biochem.*, **298**, 231–240.
26. Hawkins, M.E. (2001) Fluorescent pteridine nucleoside analogs: a window on DNA interactions. *Cell Biochem. Biophys.*, **34**, 257–281.
  27. Godde, F., Aupeix, K., Moreau, S. and Toulmé, J.J. (1998) A fluorescent base analog for probing triple helix formation. *Antisense Nucleic Acid Drug Dev.*, **8**, 469–476.
  28. Godde, F., Toulmé, J.J. and Moreau, S. (1998) Benzoquinazoline derivatives as substitutes for thymine in nucleic acid complexes. Use of fluorescence emission of benzo[g]quinazoline-2,4-(1H,3H)-dione in probing duplex and triplex formation. *Biochemistry*, **37**, 13765–13775.
  29. Godde, F., Toulmé, J.J. and Moreau, S. (2000) 4-amino-1H-benzo[g]quinazoline-2-one: a fluorescent analog of cytosine to probe protonation sites in triplex forming oligonucleotides. *Nucleic Acids Res.*, **28**, 2977–2985.
  30. Liu, C.H. and Martin, C.T. (2001) Fluorescence characterization of the transcription bubble in elongation complexes of T7 RNA polymerase. *J. Mol. Biol.*, **308**, 465–475.
  31. Wu, P.G., Nordlund, T.M., Gildea, B. and McLaughlin, L.W. (1990) Base stacking and unstacking as determined from a DNA decamer containing a fluorescent base. *Biochemistry*, **29**, 6508–6514.
  32. Rossomando, E.F., Jahngen, J.H. and Eccleston, J.F. (1981) Formycin 5'-triphosphate, a fluorescent analog of ATP, as a substrate for adenylate cyclase. *Proc. Natl Acad. Sci. USA*, **78**, 2278–2282.
  33. Scopes, D.I.C., Barrio, J.R. and Leonard, N.J. (1977) Defined dimensional changes in enzyme cofactors: fluorescent stretched-out analogs of adenine nucleotides. *Science*, **195**, 296–298.
  34. Berry, D.A., Jung, K.Y., Wise, D.S., Sercel, A.D., Pearson, W.H., Mackie, H., Randolph, J.B. and Somers, R.L. (2004) Pyrrolo-dC and pyrrolo-C: fluorescent analogs of cytidine and 2'-deoxycytidine for the study of oligonucleotides. *Tetrahedron Lett.*, **45**, 2457–2461.
  35. Tolman, G.L., Barrio, J.R. and Leonard, N.J. (1974) Chloroacetaldehyde-modified dinucleoside phosphates: dynamic fluorescence quenching and quenching due to intramolecular complexation. *Biochemistry*, **13**, 4869–4878.
  36. Wilhelmsson, L.M., Sandin, P., Holmén, A., Albinsson, B., Lincoln, P. and Nordén, B. (2003) Photophysical characterization of fluorescent DNA base analogue, tC. *J. Phys. Chem., B*, **107**, 9094–9101.
  37. Wilhelmsson, L.M., Holmén, A., Lincoln, P., Nielsen, P.E. and Nordén, B. (2001) A highly fluorescent DNA base analogue that forms Watson-Crick base pairs with guanine. *J. Am. Chem. Soc.*, **123**, 2434–2435.
  38. Eldrup, A.B., Nielsen, B.B., Haaima, G., Rasmussen, H., Kastrup, J.S., Christensen, C. and Nielsen, P.E. (2001) 1,8-Naphthyridin-2(1H)-ones: novel bicyclic and tricyclic analogues of thymine in peptide nucleic acids (PNAs). *Eur. J. Org. Chem.*, 1781–1790.
  39. Lin, K.Y., Jones, R.J. and Matteucci, M. (1995) Tricyclic 2'-deoxycytidine analogs: syntheses and incorporation into oligodeoxynucleotides which have enhanced binding to complementary RNA. *J. Am. Chem. Soc.*, **117**, 3873–3874.
  40. Lin, K.Y. and Matteucci, M.D. (1998) A cytosine analogue capable of clamp-like binding to a guanine in helical nucleic acids. *J. Am. Chem. Soc.*, **120**, 8531–8532.
  41. Rajeev, K.G., Maier, M.A., Lesnik, E.A. and Manoharan, M. (2002) High-affinity peptide nucleic acid oligomers containing tricyclic cytosine analogues. *Org. Lett.*, **4**, 4395–4398.
  42. Engman, K.C., Sandin, P., Osborne, S., Brown, T., Billeter, M., Lincoln, P., Nordén, B., Albinsson, B. and Wilhelmsson, L.M. (2004) DNA adopts normal B-form upon incorporation of highly fluorescent DNA base analogue tC: NMR structure and UV-V is spectroscopy characterization. *Nucleic Acids Res.*, **32**, 5087–5095.
  43. Roth, B. and Hitchings, G.H. (1961) 5-Arylthiopyrimidines. II. 2- and 4-Alkylamino and 4-amino derivatives. *J. Org. Chem.*, **26**, 2770–2778.
  44. Roth, B. and Schloemer, L.A. (1963) 5-Arylthiopyrimidines. III. Cyclization of 4-hydroxy derivatives to 10H-pyrimido[5,4-b][1,4]benzothiazines (1,3-diazaphenothiazines). *J. Org. Chem.*, **28**, 2659–2672.
  45. Rolland, V., Kotera, M. and Lhomme, J. (1997) Convenient preparation of 2-deoxy-3,5-di-O-p-toluoyl-alpha-D-erythro-pentofuranosyl chloride. *Synth. Com.*, **27**, 3505–3511.
  46. Brown, T. and Brown, D.J.S. (1992) Purification of synthetic DNA. *Methods Enzymol.*, **211**, 20–35.
  47. Dawson, R.M.C., Elliot, D.C., Elliot, W.H. and Jones, K.M. (1986) *Data for Biochemical Research*. Oxford University Press, NY.
  48. Morris, J.V., Mahaney, M.A. and Huber, J.R. (1976) Fluorescence quantum yield determinations: 9,10-diphenylanthracene as a reference standard in different solvents. *J. Phys. Chem.*, **80**, 969–974.
  49. Kelley, S.O. and Barton, J.K. (1998) DNA-mediated electron transfer from a modified base to ethidium: pi-stacking as a modulator of reactivity. *Chem. Biol.*, **5**, 413–425.
  50. Steenken, S. and Jovanovic, S.V. (1997) How easily oxidizable is DNA? One-electron reduction potentials of adenosine and guanosine radicals in aqueous solution. *J. Am. Chem. Soc.*, **119**, 617–618.
  51. Strickler, S.J. and Berg, R.A. (1962) Relationship between absorption intensity and fluorescence lifetime of molecules. *J. Chem. Phys.*, **37**, 814–822.
  52. Bloomfield, V.A., Crothers, D.M. and Tinoco, I. (1999) *Nucleic Acids; Structures, Properties, and Functions*. University Science Books, Sausalito, CA.
  53. Larsen, O.F.A., van Stokkum, I.H.M., Gobets, B., van Grondelle, R. and van Amerongen, H. (2001) Probing the structure and dynamics of a DNA hairpin by ultrafast quenching and fluorescence depolarization. *Biophys. J.*, **81**, 1115–1126.
  54. Reynisson, J. and Steenken, S. (2005) One-electron reduction of 2-aminopurine in the aqueous phase. A DFT and pulse radiolysis study. *Phys. Chem. Chem. Phys.*, **7**, 659–665.
  55. Seidel, C.A.M., Schulz, A. and Sauer, M.H.M. (1996) Nucleobase-specific quenching of fluorescent dyes. I. Nucleobase one-electron redox potentials and their correlation with static and dynamic quenching efficiencies. *J. Phys. Chem.*, **100**, 5541–5553.